Cell Tissue Res (2006) 326:737–748
DOI 10.1007/s00441-006-0218-0

REGULAR ARTICLE

On the atrophy of the internal carotid artery in capybara

Caroline Steele · Emerson T. Fioretto · Tais H. C. Sasahara · Wanderley L. Guidi · Ana R. de Lima · Antonio A. C. M. Ribeiro · Andrzej Loesch

Received: 16 November 2005 / Accepted: 11 April 2006 / Published online: 7 July 2006

Abstract Capybara might be a useful model for studying changes in cerebral circulation as the natural atrophy of the internal carotid artery (ICA) occurs in this animal at maturation. In this study, confocal and electron microscopy combined with immunohistochemical techniques were applied in order to reveal the changes in morphology and innervation to the proximal part of ICA in young (6-month-old) and mature (12-month-old) capybaras. Some features of the basilar artery (BA) were also revealed. The ICA of young animals degenerated to a ligamentous cord in mature animals. Immunolabelling positive for pan-neuronal marker protein gene product 9.5 but negative for tyrosine hydroxylase was observed in the proximal part of ICA at both ages examined. Axon varicosities positive for synaptophysin were present in the adventitia of ICA of young animals but were absent in the ligamentous cord of mature animals. In the ICA of young animals, adventitial connective tissue invaded the media suggesting that the process of regression of this artery began within the first 6 months of life. An increase in size of the BA was found in mature animals indicating increased blood flow in the vertebro-basilar system, possibly making capybara susceptible to cerebrovascular pathology (e.g. stroke). Capybara may therefore provide a natural model for studying adaptive responses to ICA regression/occlusion.

Keywords Internal carotid artery · Atrophy · Structure · Innervation · Capybara

The financial support of the Graduate Fund, UCL, London, UK (C. Steele) and the Brazilian Conselho Nacional de Desenvolvimento Cientifico e Tecnologico (CNPQ) Brazil (200516/01-9; A.A.C.M. Ribeiro) is gratefully acknowledged.

C. Steele · A. Loesch (✉)
Department of Anatomy and Developmental Biology,
Hampstead Campus,
Royal Free and University College Medical School,
University College London,
Rowland Hill Street,
London NW3 2PF, UK
e-mail: a.loesch@medsch.ucl.ac.uk

E. T. Fioretto · T. H. Sasahara · W. L. Guidi · A. R. de Lima · A. A. Ribeiro
Department of Surgery, College of Veterinary Medicine,
University of São Paulo (USP),
Av. Prof. Dr. Orlando Marques de Paiva,
87 São Paulo-SP, Brazil

Introduction

The capybara, *Hydrochoerus hydrochaeris*, is the largest living rodent known to man and weighs between 30 and 70 kg. It lives wild in swamp areas of South American countries including Argentina, Brazil and Colombia and is also farmed for meat and skin. Its life span in the wild is around 10–14 years (Herrera and McDonald 1984).

In most mammals blood is supplied to the anterior brain via the internal carotid artery (ICA) and to the posterior brain via the basilar artery (BA) or vertebro-basilar system (Bugge 1971; Gillilan 1972; Afifi and Bergman 1998). A study by Reckziegel et al. (2001) has shown that, in adult capybaras, this is not the case; instead, the entire brain blood supply travels via the vertebro-basilar system (type III according to de Vriese classification; de Vriese 1905; Reckziegel et al. 2001, 2004). Moreover, in place of the ICA, a fine fibrous cord (or ligamentous cord) has been observed. The presence of this cord suggests that the ICA must have been functional during ontogeny (Reckziegel et al. 2001), although the timing of the formation of the cord is unclear.

The possibility has arisen from a study by Islam et al. (2004) that the cerebral vasculature of the capybara might

undergo remodelling during animal maturation. Islam et al. (2004) have reported that smooth muscle cells resembling macrophages or monocytes can be seen in the BA of 1-year-old animals and suggest that these are associated with remodelling of the artery following regression of the ICA.

The ICA and BA of mammals serve as conduits for sympathetic nerves innervating individual cerebral blood vessels (Weninger and Muller 1997; Simons and Ruskell 1988; Suzuki et al. 1988). Sympathetic nerves supplying the middle cerebral artery (MCA), the anterior cerebral artery (ACA) and its branches and part of the BA have their cell bodies in the superior cervical ganglion (Tamamaki and Nojyo 1987; Handa et al. 1990). Sympathetic nerve fibres supplying the cerebral vasculature of the more posterior regions of the brain have their cell bodies in the stellate ganglion (Arbab et al. 1988). In addition, cerebral blood vessels are parasympathetically innervated by nerves originating in the cranial sphenopalatine, otic, carotid, pterygopalatine and cavernous sinus ganglia (Suzuki et al. 1988; Edvinsson et al. 1989; Bleys et al. 2001) and are innervated by sensory nerves from the trigeminal, internal carotid and first and second cervical spinal ganglia (Arbab et al. 1986; Hardebo et al. 1989). The types of nerves (if any) that project via the ICA to the cerebral vessels of capybara are unknown. If they are present, an important question regarding these nerves, and the sympathetic nerves in particular because of their protective role (Sadoshima et al. 1981; Sadoshima and Heistad 1982; Coutard et al. 2003), is their fate when this artery degenerates. The autonomic ganglia innervating cerebral blood vessels in mammals have been shown to be involved in a variety of physiological functions (Cardinali et al. 1981; Thrasivoulou and Cowen 1995) and are therefore known to be important in health and disease (Owman and Edvinsson 1977; Boydell 1995; Bell et al. 2001). In the case of capybara, no data are as yet available with respect to the precise role of the ganglia and their participation in the innervation of the cerebral vascular bed.

The capybara may potentially be a good model for studying the mechanisms of changes in the cerebral vascular bed, as the regression of the ICA occurs at sexual maturity (Reckziegel et al. 2001). This regression is likely to lead to the vertebro-basilar system being overloaded and to many vascular and/or neurovascular changes. Study of these changes is important as the capybara has cerebral vessels allometrically closer to man than those of the smaller rodents frequently used for such research (see Gladstone et al. 2002; Fisher and Ratan 2003; Lindner et al. 2003). As capybaras are farmed for meat (under relevant licensing), their brains and cerebral vasculatures can readily be obtained for research. Recent studies on the structure of BA and the distribution of endothelin-1 and its receptors in this vessel have taken advantage of the farming of capybaras in Brazil and have contributed to our knowledge of the make-up of cerebral vasculature in these animals (Islam et al. 2004; Loesch et al. 2005). However, little is known about the microanatomy of the cerebral vessels during regression of the ICA.

The aim of the present study has therefore been to investigate the morphology of the ICA in young and mature capybaras. In particular, we have focused on revealing: (1) general morphological features of the ICA in young animals, (2) changes in the ICA-ligamentous cord associated with atrophy of the artery during capybara maturation, and (3) general aspects of the innervation to the ICA/ligamentous cord by using immunohistochemical labelling. We have also examined general changes in size of the BA during atrophy of the ICA.

Materials and methods

Eight 6-month-old (young) and eight 12-month-old (mature) female capybaras were used in this study. Tissue samples were obtained from the Profauna Farm in São Paulo, Brazil, under a licence granted by the Brazilian Institute of the Environment - IBAMA (1-35-93-0848-0). Animals were killed by using an overdose of pentobarbitone, which was administered intravenously at 80 mg/kg. The jugular vein was then opened to allow perfusion-fixation (~500 ml fixative) of the cerebral vasculature via a cannula inserted into the left common carotid artery. For electron microscopy including electron immunocytochemistry, the fixative consisted of 4% formaldehyde and 0.2% glutaraldehyde in 0.1 M phosphate buffer (pH 7.4), whereas for the fluorescence-confocal immunohistochemistry, the fixative consisted of 4% formaldehyde (in phosphate buffer) without glutaraldehyde. In all animals examined, the proximal part of left ICA, just after its origin from the common carotid artery in the neck, and also the BA (for measurement purposes) were dissected out and placed in the same fixative overnight at 4°C. Because of lack of accessibility, no samples were taken from the intracranial or terminal part of ICA. Specimens were then transferred to the 0.1 M phosphate buffer containing 0.1% sodium azide and stored at 4°C until processed for morphological and immunohistochemical examination at the electron- and fluorescence-confocal microscopic levels; semithin sections of standard electron-microscopic preparations were also examined at the light-microscopic level.

Light and standard electron microscopy: semithin and ultrathin sections

Specimens of the ICA and the ICA-ligamentous cord (left middle part) were (1) washed in 0.1 M sodium cacodylate

buffer (pH 7.4), (2) postfixed for 1 h at 4°C in 1% osmium tetroxide (in sodium cacodylate buffer), (3) washed in sodium cacodylate buffer, (4) *en block* stained with a 2% solution of uranyl acetate in distilled water, (5) dehydrated in a graded ethanol series and (7) embedded in Araldite blocks for polymerisation. Semithin sections (1.5 μm) of the ICA and ICA-cord were cut from the Araldite blocks by using an Ultracut E Reichert-Jung microtome, stained with toluidine blue and subsequently examined by using a Zeiss Axioplan microscope (Zeiss, Germany). Optical images obtained with a Leica DC200 digital camera were stored digitally for examination. Ultrathin sections (~80 nm) of the specimens were also cut from the Araldite blocks on the same microtome, stained with uranyl acetate and lead citrate and subsequently examined and photographed with a JEOL-1010 transmission electron microscope (TEM).

Fluorescence-confocal immunohistochemistry of protein gene product 9.5 and tyrosine hydroxylase

To study the general aspects of innervation to the ICA and ICA-ligamentous cord, including the sympathetic innervation, antibodies were used to detect (1) the general neuronal marker, protein gene product 9.5 (PGP), which is a marker for all types of nerves (Thompson et al. 1983), and (2) tyrosine hydroxylase (TH), the rate-limiting enzyme in noradrenaline synthesis in sympathetic nerves (Pickel et al. 1975). Specimens were washed in phosphate buffer and infiltrated overnight at 4°C with cryoprotectant consisting of 25% sucrose and 10% glycerol (by volume, in 0.1 M phosphate buffer at pH 7.4). They were then embedded in OCT compound (BDH/Merk, Leicester, UK) and frozen in pre-cooled (by liquid nitrogen) isopentane. The ICA and ICA-ligamentous cord were systematically and uniformly cross-sectioned at 50 μm along the whole length of the specimen by using a Reichert-Jung CM1800 cryostat and collected in phosphate-buffered saline (PBS) for the immunoprocedures. After being washed for 30 min in PBS containing 0.1% Triton, sections were (1) placed for 1 h in 10% non-immune normal horse serum (Nordic Immunology, Tilburg, The Netherlands, (2) incubated for 24–48 h with a rabbit polyclonal antibody to PGP diluted 1:1,500 in PBS containing 5% non-immune normal horse serum, 0.1% DL-lysine and 0.1% sodium azide, (3) washed in PBS, (4) incubated for 2 h with a biotin-conjugated donkey anti-rabbit IgG serum (Jackson ImmunoResearch Laboratories, West Grove, Pa., USA) diluted 1:500 in PBS, (5) washed in PBS, (6) exposed for 2 h to streptavidin labelled with fluorescein isothiocyanate (Streptavidin-FITC; Jackson ImmunoResearch) diluted 1:200 in PBS, (7) washed in PBS and (8) further processed for tyrosine hydroxylase (TH) immunoreactivity to detect sympathetic neurons (Pickel et al. 1975). This process included (1) incubation for 1 h in 5% non-immune normal goat serum (Nordic Immunology), (2) incubation for 24–48 h with a mouse monoclonal antibody to TH diluted 1:500–1,000 in PBS containing 1% non-immune normal goat serum, 0.1% DL-lysine and 0.1% sodium azide, (3) washes in PBS, (4) incubation for 3 h with a biotin-conjugated goat anti-mouse IgG serum (Jackson ImmunoResearch) diluted 1:500 in PBS, (5) washes in PBS, (6) exposure for 2 h or overnight to streptavidin-Texas red (Amersham, Biosciences, Little Chalfont, UK) diluted 1:200 in PBS, (7) washes in PBS and then (8) immediate mounting in Citifluor for examination with a confocal laser microscope (Leica DMRBE microscope with SPZ confocal head and Leica confocal software). Fluorescence filters allowed the discrimination of labelling with FITC (488 excitation line) and Texas red (568 excitation line); objective lenses (×10 and ×20, dry aperture; ×40 and ×63, oil immersion) were used for examination of the specimens. Consecutive individual images were collected at 1.5-μm intervals and stored digitally for subsequent analysis. The images were merged as overlays or maximal projections.

Electron immunocytochemistry of synaptophysin

To identify perivascular nerve varicosities, we used a specific antibody to synaptophysin, which is an integral membrane glycoprotein of presynaptic vesicles (Weidenman and Frank 1985; Navone et al. 1986). Fixed specimens of the ICA/ligamentous cord were washed in phosphate buffer and then in 0.1 M TRIS-buffered-saline (TBS), at pH 7.6. Cross sections of the artery (~100 μm thick) were cut by using a vibratome (Technical Product International, St. Louis, USA), collected in TBS and immunoprocessed (at room temperature) for electron microscopy. In brief, sections were (1) exposed to 0.3% hydrogen peroxide in 33% ethanol for 45 min (in order to block endogenous peroxidases), (2) washed in TBS, (3) placed for 1 h in 10% non-immune normal horse serum (Nordic Immunology), (4) washed in TBS, (5) incubated for 48 h with a rabbit polyclonal antibody to synaptophysin diluted 1:1,000 in TBS containing 10% non-immune normal horse serum and 0.1% sodium azide, (6) washed in TBS, (7) incubated for 12 h with a biotin-conjugated donkey anti-rabbit IgG serum (Jackson ImmunoResearch) diluted 1:500, (8) washed in TBS, (9) exposed for 5 h to ExtrAvidin-horseradish peroxidase conjugate (Sigma, Poole, UK) diluted 1:1,500 in TBS and (10) washed in TBS. Immunoreactivity was visualised with 3,3'-diaminobenzidine (Sigma) in TBS containing 0.01% H_2O_2. After extensive rinses with TBS and distilled water, sections were placed for 1 h at 4°C in 1% osmium tetroxide (in 0.1 M sodium cacodylate buffer) and dehydrated through a graded ethanol series followed by propylene

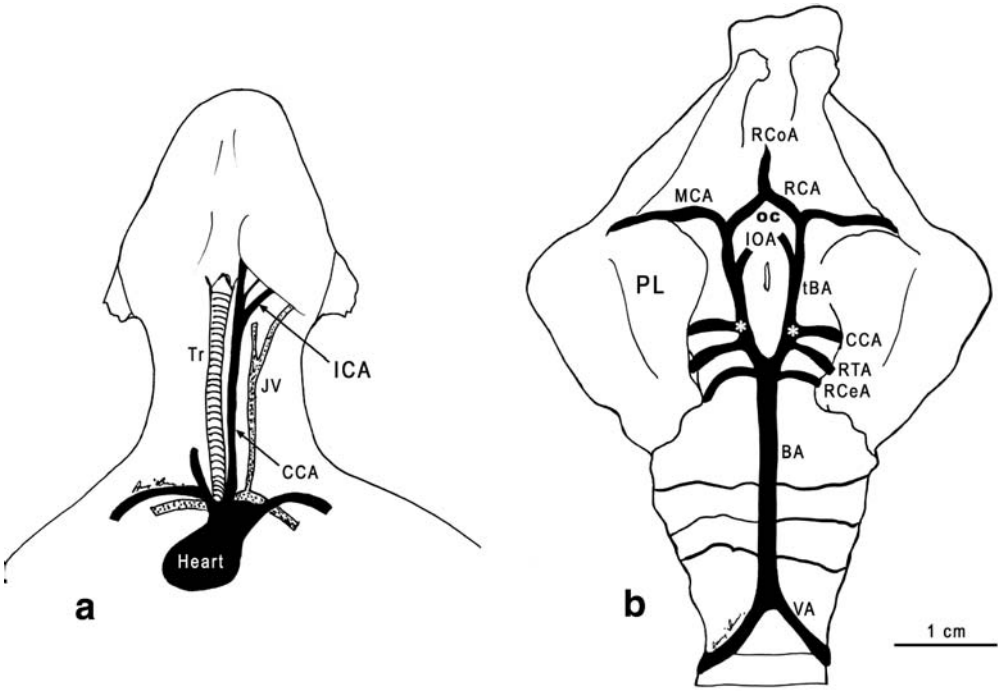

Fig. 1 **a** Representation of ICA in the neck of an adult capybara (*Tr* trachea, *JV* jugular vein, *CCA* common carotid artery, *ICA* internal carotid artery). **b** Representation of the brain-base arterial system in an adult capybara (*VA* vertebral artery, *BA* basilar artery, *RceA* rostral cerebellar artery, *RTA* rostral tectal artery, *CCA* caudal cerebral artery, *tBA* terminal branch of the BA, *IOA* internal ophthalmic artery, *RCA* rostral cerebral artery, *MCA* middle cerebral artery, *RcoA* rostral communicating artery, *OC* optic chiasm, *PL* piriform lobe, *asterisks* possible sites of complete mergence of ICA with the left and right *tBA* at the region of origin of *CCA*; see Reckziegel et al. 2001). *Bar* 1 cm (brain only)

oxide. Specimens were flat embedded in Araldite, between two sheets of melinex, and polymerised. Areas of interest were then selected, cut out and attached (by superglue) to Araldite blocks for ultrathin and semithin sectioning. Sections were examined and photographed as described above by using a JEOL-1010 TEM (for ultrathin sections) and a Zeiss Axioplan microscope with Leica DC200 digital camera (for semithin section).

Antibodies and immunohistochemical controls

PGP polyclonal antibody (RA95101: UltraClone Limited, Wellow, Isle of Wight, UK) was raised in rabbit against human PGP 9.5 protein purified from a pathogen-free human brain. This antibody cross-reacts with PGP 9.5 in mammals; it labels neuronal cell bodies and axons in the central and peripheral nervous systems, including fine

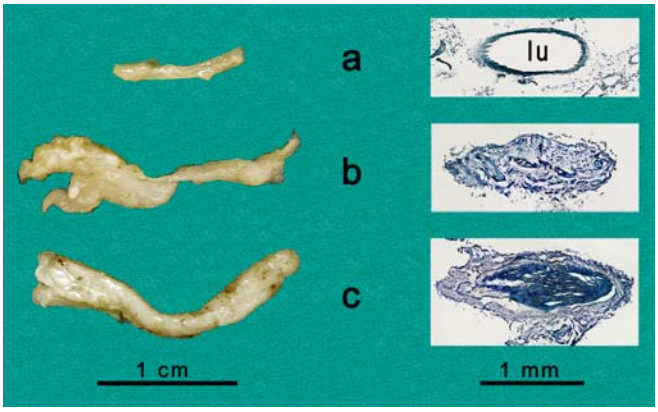

Fig. 2 General morphological features of the proximal part of ICA. *Left* Specimens from 6-month-old (**a**), 12-month-old (**b**) and 2-year-old (**c**) capybaras showing progression of artery occlusion with age. *Right* Cryostat cross sections (18 μm thick; lightly stained with toluidine blue) of the relevant arteries *left*. Note the open lumen (*lu*) of ICA in **a** and the progression of lumenal occlusion by fibrous tissue in **b**, **c**

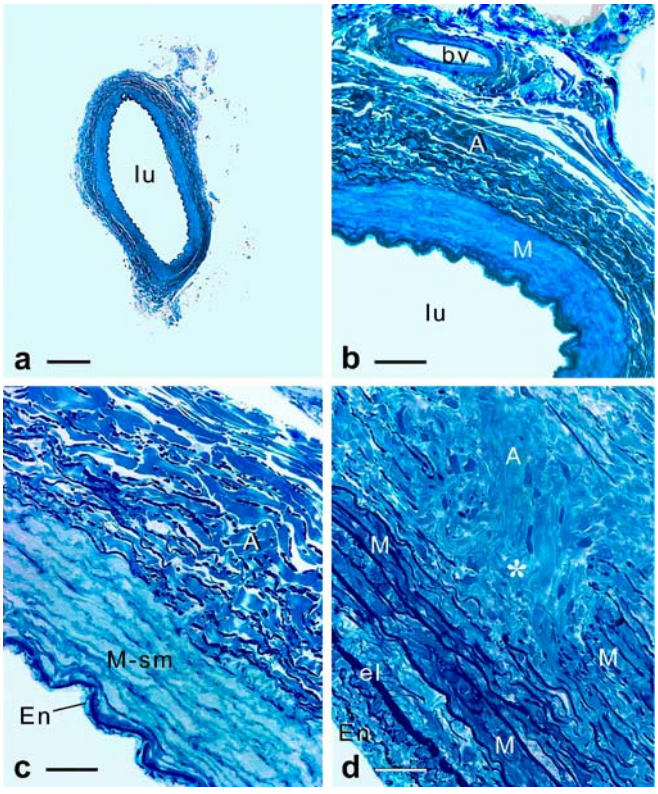

Fig. 3 ICA of 6-month-old capybara: semithin cross sections stained with toluidine blue. **a** General view of the artery (*lu* lumen). **b** In the ICA wall, note the media/smooth muscle (*M*) and adventitia/connective tissue (*A*), which also supports a small blood vessel (*bv*). **c** Higher magnification of the ICA showing intima/endothelium (*En*), compact layers of medial smooth muscle cells (*M-sm*) and adventitia/connective tissue (*A*). **d** Note local disruption to the media: invasion of adventitial connective tissue (*asterisk*) into the media; bundles of elastin can also be seen (*dark blue parallel strands*). Endothelium (*En*), internal elastic lamina (*el*), media/smooth muscle (*M*) and adventitia/connective tissue (*A*) are clearly present. *Bars* 200 μm (**a**), 50 μm (**b**), 25 μm (**c, d**)

nerve fibres in peripheral tissues (UltraClone). TH monoclonal antibody (type IgG1, T-2928; Sigma, St. Louis, Mo., USA) was derived from TH-16 hybridoma cells produced by fusion of mouse myeloma cells and splenocytes from immunised BALB/c mice. Purified rat TH was used as the immunogen. The antibody recognises TH in numerous mammalian species including man, monkey, cow, sheep, rabbit, guinea pig and rat (Sigma). Synaptophysin polyclonal antibody (A010: DAKO, Glostrup, Denmark) was an affinity-isolated antibody raised in rabbit against synthetic human synaptophysin peptide coupled to ovalbumin. The antibody was shown to react with neurones in the brain, spinal cord and retina and with neuroendocrine cells (e.g. of adrenal medulla, carotid body or pituitary gland; DAKO). For all antibodies, routine immunolabelling controls were applied with omission of the primary antibody and IgG steps, independently.

Measurements

Measurements of the ICA were made by using a Leitz Wetzlar (Germany) light microscope, a graticule (Graticules, London) and dry objectives; ×10, ×20 or ×40. The outer (adventitial) and inner (lumenal) diameters of the ICA were measured on 100-μm-thick Araldite flat-embedded vibratome cross sections of the artery. Two measurements at right angles to each other were taken from each section (×10 or ×20 objectives). The thickness of the adventitia and media was estimated by measurement in four different regions, opposite to each other, for each semithin section; five 1.5-μm toluidine-blue-stained semithin sections were used from each ICA or ICA-ligamentous cord from each animal. Measurements were also made on Araldite-embedded cross sections of the middle part of the BA (vibratome sections as described above for ICA). The measurements from five ICA and five ICA-ligamentous cords or three BA for each animal group (6- and 12-month-old capybaras) are presented as mean values (±SD).

Results

To elucidate the source of the blood supply to the brain of capybara, we examined the anatomy of the brain-base arterial system and the general morphological features of the proximal part of ICA in young and mature species (Figs. 1, 2).

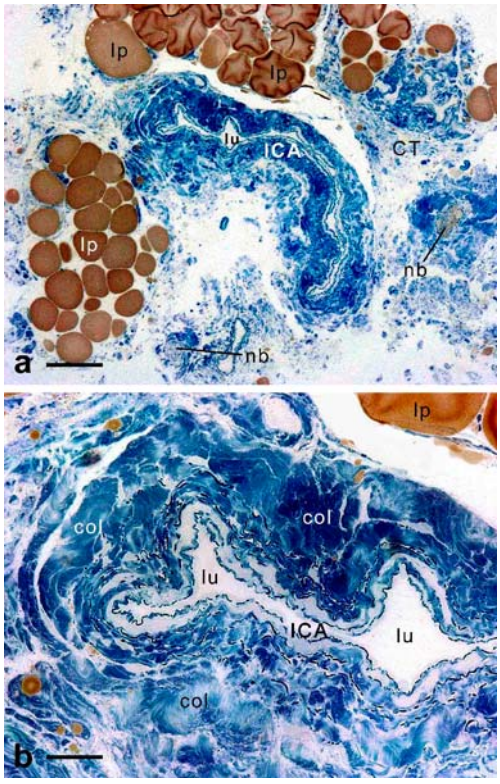

Fig. 4 Light microscopy of ICA-ligamentous cord of 12-month-old capybaras: semithin cross sections stained with toluidine blue. **a** Note that the redundant ICA (*ICA*) with its collapsed lumen (*lu*) is "embedded" in the cord, which is rich in connective tissue (*CT*) including fat cells filled with lipids (*lp*). Two nerve bundles (*nb*) lie within the connective tissue. **b** At higher magnification, an abundance of collagen bundles (*col*) can be seen around the collapsed lumen (*lu*) of the ICA. *Bars* **a** 100 μm, **b** 25 μm

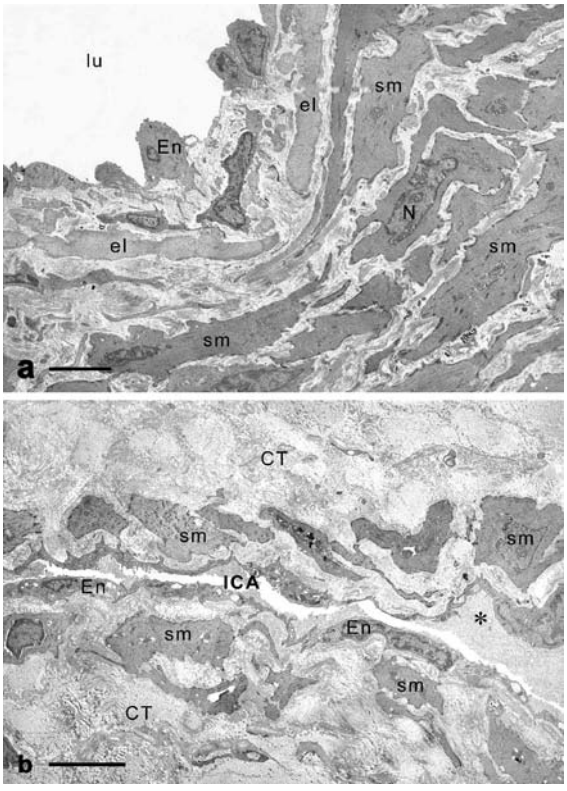

Fig. 5 Standard electron microscopy of ICA and ICA-ligamentous cord of 6-month-old (**a**) and 12-month-old (**b**) capybaras. **a** Note the intimal endothelium (*En*) lining the lumen (*lu*); the media is composed of several layers of smooth muscle cells (*sm*). Note the nucleus (*N*) of a smooth muscle cell and the internal elastic lamina (*el*). **b** The lumen is reduced to a narrow elongated space (*ICA*) lined by flattened endothelial cells (*En*). The media is reduced to 1 or 2 layers of smooth muscle cells (*sm*) loosely embedded in adjacent connective tissue (*CT*). Precipitated blood proteins (*asterisk*) are also visible. *Bars* 5 μm

Light microscopy of ICA and ICA-cord

Young animals

Examination of the ICA from 6-month-old animals at the light-microscopic level revealed that this artery had all the characteristic features of an arterial vessel. The lumen was wide open and the intima (endothelium), media (vascular smooth muscle cells; VSMCs) and adventitia (connective tissue) were all distinct (Fig. 3a,b). Several layers of VSMCs could be seen in the media (Fig. 3c). In some sections of the ICA, the adventitial connective tissue clearly invaded the media (Fig. 3d).

Mature animals

Macroscopic examination of 12-month-old capybaras revealed the presence of a ligamentous cord instead of the ICA. Light microscopy of semithin sections of the ligamentous cord showed that the ICA lumen was reduced to a narrow elongated space embedded in extensive connective tissue consisting of collagen and fat cells (Fig. 4a,b). The intima of ICA comprised of endothelial cells, but no VSMCs of the media could be seen at this level of magnification. A few nerve bundles of various sizes were seen in the connective tissue neighbouring the reduced ICA (Fig. 4a).

ICA and ICA-cord measurement

Measurement of the ICA of young animals showed that the external diameter of the artery was (mean±SD) 1.97±0.58 mm (n=5) and the internal diameter was 1.41±0.66 mm (n=5). The thickness of the artery wall (thickness of intima, media and adventitia taken together) was therefore around 0.56 mm. In mature animals, the external diameter of the ICA-ligamentous cord was 1.98±0.34 mm (n=5).

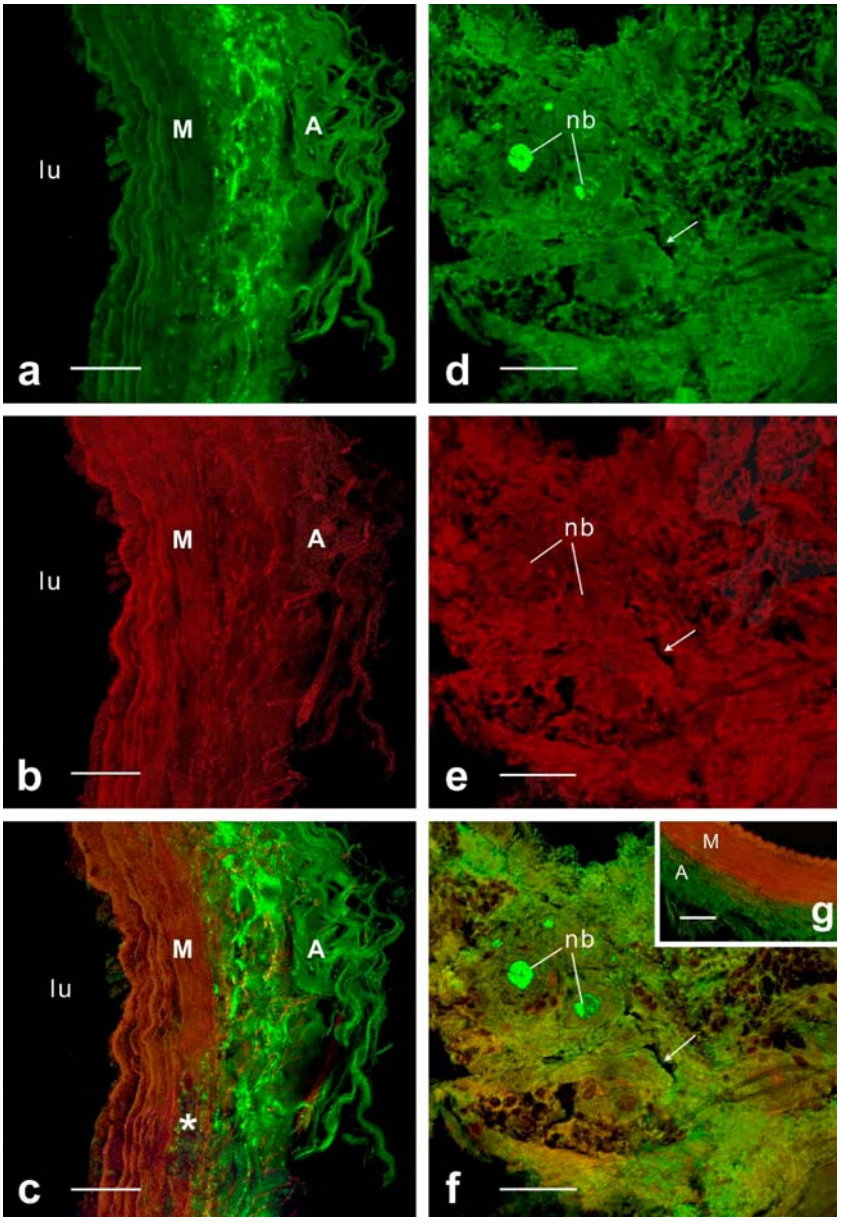

Fig. 6 Fluorescence confocal microscopy of ICA and ICA-ligamentous tissue of 6-month-old (**a–c, g**) and 12-month-old (**d–f**) capybaras. **a, d** Immunolabelling for PGP (*greenish-yellow*) reveals the plexus of perivascular autonomic innervation (note its fragmented pattern) to the ICA in young animals, whereas only large diameter PGP-positive nerve bundles (*nb*) are seen in the ICA-ligamentous tissue of mature animals (*arrow* redundant ICA, *A* adventitia, *M* media, *lu* lumen). **b**, **e** No labelling (*bright red*) for TH. **c**, **f** Hence, no colocalisation of PGP and TH. Note that, in **c**, the adventitia can also be seen invading into media (*asterisk*). **g** An example of ICA processed for control immunolabelling with omission of PGP and TH antibodies; neither labelling for PGP nor for TH can be seen in the overlay image of the artery. *Bars* 50 μm (**a–c, g**), 250 μm (**d–f**)

Standard electron microscopy of ICA

Young animals

By electron-microscopic examination, the ICA of 6-month-old capybaras was again seen to have classic arterial organisation (Fig. 5a). The intima and media were well structured, and the internal elastic lamina separating them was well defined. VSMCs had a mostly circular orientation and small bands of elastin and collagen fibres could be seen between them. Endothelial cells often protruded to varying extents into the lumen of the artery; these protrusions usually included the cell nucleus. The adventitial connective tissue was extensive, being rich in thick collagen bundles and fibroblast processes (data not shown).

Mature animals

At the electron-microscopic level, the lumen of ICA of 12-month-old capybaras could be seen to be reduced to a

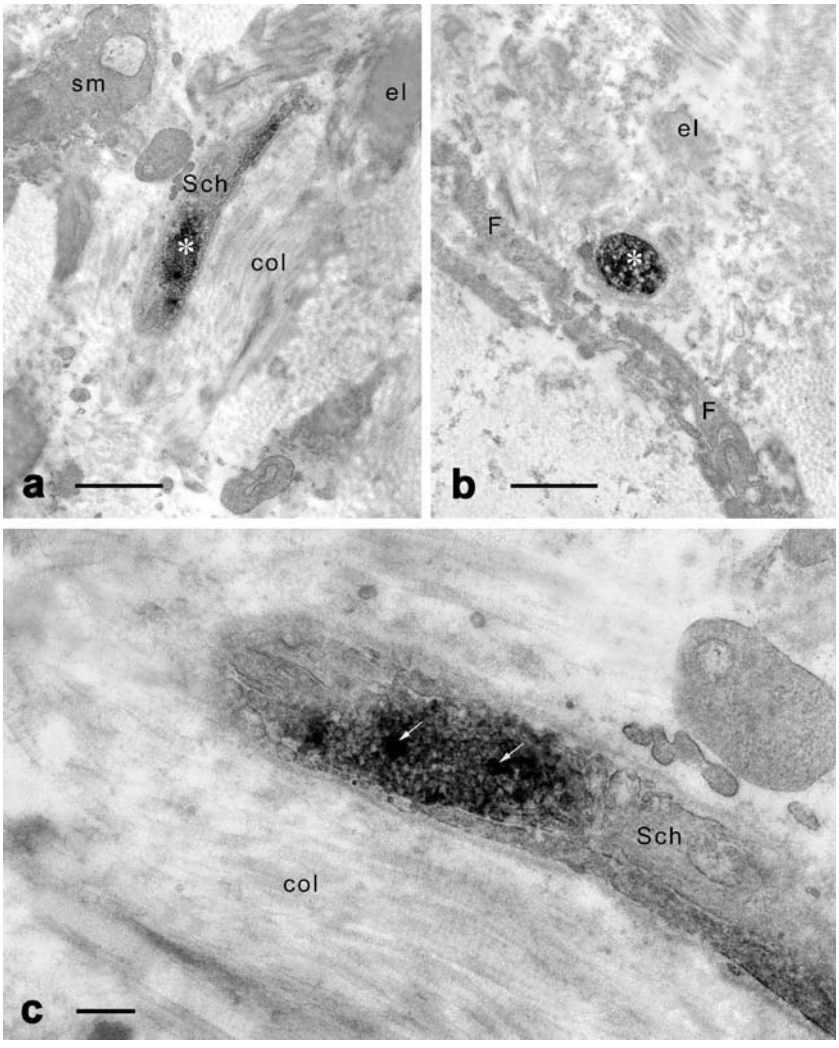

Fig. 7 Electron microscopy of ICA of 6-month-old animals. **a** Extensive adventitia displaying an axon immunoreactive for synaptophysin (*asterisk*). A smooth muscle cell (*sm*), elastin (*el*), collagen (*col*) and Schwann cell (*Sch*) can be seen. **b** An axon positive for synaptophysin in cross-section (*F* fibroblast). **c** Magnified axon varicosity shown in **a** exhibiting granular and agranular synaptic vesicles (*arrows*). *Bars* 1 μm (**a, b**), 200 nm (**c**)

narrow elongated space (cf. light-microscopic results). The arrangement of the three vascular layers (intima, media and adventitia) greatly differed from that of the young animals. The intima consisted of flattened endothelial cells, whereas the media consisted of only one or two layers of VSMCs embedded in connective tissue; beyond this, much fibrous connective tissue was present (Fig. 5b).

Fluorescence-confocal microscopy of PGP (9.5) and TH

Young animals

The perivascular autonomic innervation to the ICA of young animals was examined by using immunolabelling for PGP (Fig. 6a). PGP-positive nerve fibres of various diameters were present in the adventitial layer. The pattern of these fibres was fragmented. No obvious immunoreactivity for TH was observed (Fig. 6b) and therefore no co-localisation with PGP was visible (Fig. 6c). Again, in some regions of ICA, the adventitia could be seen to be invading the medial layer (Fig. 5c).

Mature animals

In 12-month-old animals, no perivascular nerve fibres showing immunoreactivity for PGP were observed in the close vicinity of atrophied ICA. However, larger PGP-positive nerve bundles were present (Fig. 6d). Usually two or three of these bundles could be seen in the connective tissue at some

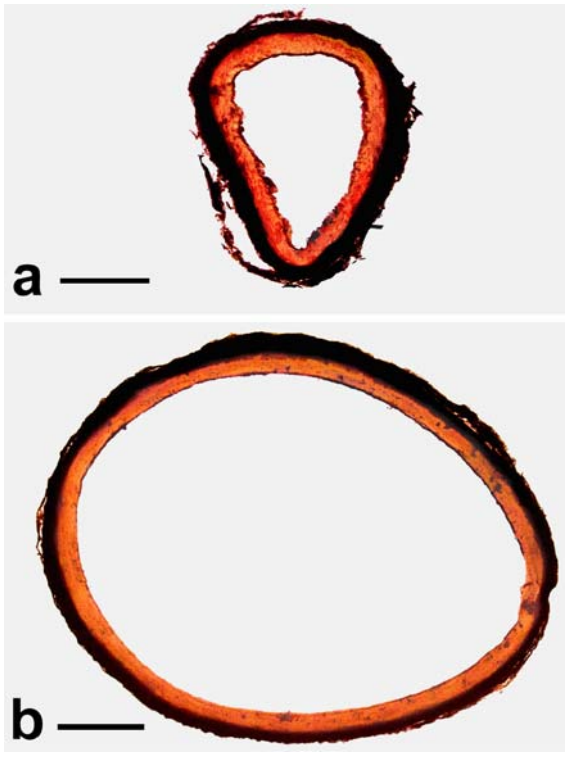

Fig. 8 Light microscopy of 100-μm-thick cross sections of BA (osmicated and embedded in Araldite) from 6-month-old (**a**) and 12-month-old (**b**) animals; the media is visible as an *orange-reddish* stain, whereas the adventitia is seen as the external dark ring. A drastic increase in the size (diameter) of the artery can be seen in the mature animal (~2.6×3.1 mm) when compared with the young animal

distance from the atrophied ICA lumen. No immunoreactivity for TH was observed (Fig. 6e) and therefore no co-localisation with PGP was observed in nerve profiles (Fig. 6f).

Immuno-fluorescence controls

No immunoreactivity for PGP or TH was observed in sections processed as immuno-fluorescence controls (Fig. 6g).

Electron immunocytochemistry of synaptophysin

Young animals

Immunolabelling for synaptophysin revealed positive axon varicosities scattered in the adventitia of young animals (Fig. 7a,b). These varicosities contained both large granular and small agranular synaptic vesicles (Fig. 7c). No juxtaposition of labelled varicosities and VSMCs was seen.

Mature animals

The ICA-ligamentous cord of all 12-month-old animals examined exhibited no axon varicosities immunoreactive for synaptophysin. The large nerve bundles that were positive for PGP by using confocal microscopy showed no immunoreactivity for synaptophysin (data not shown).

BA: general morphology

The ultrastructure of the capybara BA is that of a typical cerebral artery comprising intima, media and adventitia (Islam et al. 2004). By light microscopy, a drastic increase in the cross-sectional size of the artery was seen in the mature animals compared with young animals (Fig. 8). Measurements of BA showed that, in young animals (n=3), the external diameter of the artery was (mean±SD) 1.24±0.17 mm and the internal diameter was 0.88±0.22 mm (n=3). In mature animals (n=3), the external diameter of the artery was 2.63±0.57 mm and the internal diameter was 2.24±0.58 mm. These measurements indicated that the diameter of the BA had greatly increased (doubled) by the age of 12 months. However, in the same specimens, the thickness of the artery wall was roughly equal in young and mature animals, viz. 0.36 mm and 0.39 mm, respectively. More precise measurements (26×2 measurements) taken from semithin sections stained with toluidine blue showed the thickness of the media to be 0.14±0.03 mm (n=2) in young animals and 0.11±0.02 mm (n=2) in mature animals. The media was therefore slightly thicker in young animals.

Discussion

Atrophy of ICA

In addition to the macroscopic indications of the phenomenon of regression of the ICA in capybara (Reckziegel et al. 2001), this study has demonstrated, for the first time, the histological (microstructural) changes that occur within the ICA and its surrounding tissues as a result of this regression. Our light- and electron-microscopic results have revealed that the main function of the ICA in young (6-month-old) animals, viz. supplying blood to the anterior brain (Bugge 1971; Gillilan 1972; Afifi and Bergman 1998), is no longer performed by the ligamentous cord in mature (12-month-old) animals. The lumen is severely collapsed and the VSMC layer is almost completely replaced by connective tissue, suggesting that the blood supply by the artery is severely restricted.

This study suggests that the increased connective tissue around the atrophied lumen is derived from the original adventitia of the ICA and, in some cases in young animals, the adventitia can be seen to invade the medial smooth muscle coat. At this stage, however, the possible mechanism(s) involved in this invasion and proliferation of adventitia

around the ICA atrophied lumen is (are) unknown. In response to vascular diseases or in experimental models of vascular damage, a cascade of cytokines is known to be released stimulating various cellular responses and interactions in the vascular wall. The results of these interactions are usually the proliferation of VSMCs and the hyperplasia of the intima (Clowes et al. 1983; Casscells 1992; Ross 1993). In contrast, in the ICA of mature capybaras, atrophy of the media and a decline of VSMCs has been observed. Furthermore, no signs of VSMC degeneration or apoptotic features, e.g. nuclear condensations or membrane blebbing (Malik et al. 1998), have been observed by electron microscopy. This suggests that the process occurring in the ICA is markedly different from that which occurs when a blood vessel is damaged. Studies specifically aimed at detecting apoptotic markers might help to improve our understanding of the mechanisms of the atrophy of the ICA. Given that the adventitia can be seen invading into the media of the ICA in young capybaras, and that the pattern of innervation seems fragmented (suggesting that the nerves may be starting to degenerate), the variety of changes and processes taking place might well begin in young animals and advance to variable extents in different regions of the artery and at different ages.

Variations in the sources of blood supply to the brain of rodents including capybara have long been recognised (de Vriese 1905) and more recently described by Reckziegel et al. (2001, 2004). As far as we are aware, the precise timing and location, during embryonic development or early postnatal life, that the ICA is incorporated into the brain-base arterial system of capybara are unknown. According to Reckziegel et al. (2001), in adult capybaras (exact age not specified), the caudal terminal branch of ICA is merged completely with the left and right terminal branches of the BA from which the caudal cerebral arteries derive. Our own unpublished observations suggest the plasticity of ICA and the possible termination of the artery in the brain-base arteries. In this study, no ICA has been observed in connection with the base artery system in adults from about 12 months onwards. Specially designed studies of the whole length of ICA are required to examine artery plasticity and to clarify its vascular arrangement. These might also help to reveal the extent of the changes in the artery conduit, in particular in its less accessible cranial part, possibly occurring during embryonic and postnatal development, maturation or ageing. In relation to the plasticity of ICA system, a study of chinchillas, which have a type of blood supply to the brain similar to that of capybara (type III circulation) has shown that, in the majority of adults (~93% cases), the ICA does not contribute to encephalic irrigation. In some cases, however, the artery does not follow its usual path towards the hypophysis but reaches the BA at the level of the medulla oblongata and contributes to the entire irrigation of the base of the encephalon (Araújo and Campos 2005). In capybara, changes in ICA might be particularly crucial for this species at early stages of post-natal development.

Innervation of the ICA/ligamentous cord

Surprisingly, although perivascular nerves are present in the ICA of 6-month-old capybaras, as confirmed by the presence of immunoreactivity to PGP, they are negative for TH. The presence of axon varicosities positively immunolabelled for synaptophysin suggests that these are functioning varicosities; however, they are rare and difficult to find by standard electron microscopy, possibly because of the extensive adventitia. In the ligamentous cord of 12-month-old animals, nerve bundles immunoreactive for PGP could clearly be seen. These nerves are not associated with the perivascular region of atrophic ICA, but project elsewhere, and are immunonegative for TH. Therefore, the results obtained from both young and mature capybaras suggest a lack or partial lack of sympathetic innervation or some phenomenon affecting this innervation in the proximal part of ICA during development and/or maturation of capybara from 6 month onwards. The possibility cannot be ruled out that, during development and/or maturation, sympathetic disconnection from the superior cervical ganglion occurs at the proximal part of ICA resulting in undetectable levels of TH. Studies of rat cerebral vessels have shown that TH expression can be completely abolished by sympathectomy (Mione et al. 1991). Since only the cervical portion of ICA has been examined in the present study, no data is available concerning the innervation of the whole length of the artery. Our latest preliminary observations (which require verification) of a few cases of young capybaras (7-day-old to 1-month old) suggest the presence of TH-positive innervation in possibly the distal part of ICA contacting the middle cerebral artery arch near the optic chiasm. However, various regions of ICA in capybara might be innervated by nerves from different ganglia in a different pattern from that well defined in laboratory mammals (Arbab et al. 1986, 1988; Tamamaki and Nojyo 1987; Suzuki et al. 1988; Edvinsson et al. 1989; Hardebo et al. 1989; Handa et al. 1990; Bleys et al. 2001). Some exceptions to the normal mammalian pattern of the distribution of sympathetic nerves from the superior cervical ganglion are known. For example, in the guinea pig, which also has the type III cerebral vasculature according to the de Vriese classification (de Vriese 1905; see Reckziegel et al. 2001), there is no major communication between the ICA and the circle of Willis (Nilges 1944). Sympathetic nerves from the superior cervical ganglion may thus supply the ophthalmic artery rather than the

cerebral vessels. To examine cerebrovascular innervation in capybara in more detail, additional systematic studies including the application of neuronal tracing are now being planned in our laboratories.

BA remodelling

The BA has a much larger diameter in 12-month-old animals than in 6-month-old animals. The external and lumenal diameters more than double. This suggests a remodelling of the artery most probably attributable to an extra workload as, after regression of the ICA, the BA becomes the main artery supplying blood to the brain (Reckziegel et al. 2001). The regression of the ICA is likely to be accompanied by an increase in blood pressure in the BA and some other large arteries, e.g. the posterior communicating artery, possibly making mature capybaras prone to cerebrovascular disorders. However, the difference in size of the BAs examined might also reflect different states of contraction/relaxation of the arteries at the time of fixation. Further systematic measurements of the diameter of the BA (in fixed and non-fixed specimens) from animals of various ages should clarify this. Studies demonstrating the presence of "active" VSMCs resembling macrophages or monocytes strongly suggest that a remodelling process is taking place in the BA of mature (12-month-old) capybaras (Islam et al. 2004).

Concluding remarks

The present study has revealed morphological details associated with the atrophy of the ICA in capybara at maturation. In young 6-month-old animals, autonomic perivascular nerves with "active" varicosities innervate the ICA, although no TH-positive (sympathetic) innervation has been detected in the proximal part of the artery. The ICA-ligamentous cord in mature capybaras appears to be non-functional, whereas the diameter of the BA nearly doubles. This suggests an increased blood flow through the BA in response to the regression of the ICA. The phenomenon of regression of the ICA and the increased blood flow through the BA and the rest of the vertebrobasilar system (if this is the case) makes the capybara, potentially, a unique natural model for studying maturational remodelling of the cerebral vasculature and neuronal plasticity.

Acknowledgements We thank Mrs. Carla Ciqueira de Figueiredo Baretto and Mr. Paulo Bezerra Da SilvA (from Profauna Farm, Iguape, São Paulo, Brazil) for providing capybaras for the study.

References

Afifi AK, Bergman RA (1998) Functional Neuroanatomy. McGraw-Hill, New York

Araújo ACP, Campos R (2005) A systematic study of the brain base arteries in Chinchilla (*Chinchilla lanigera*). Braz J Morphol Sci 22:221–232

Arbab MAR, Wiklund L, Svendgaard NA (1986) Origin and distribution of cerebral vascular innervation from superior cervical, trigeminal and spinal ganglia investigated with retrograde and anterograde WGA-HRP tracing in the rat. Neuroscience 19:695–708

Arbab MAR, Wiklund L, Delgado T, Svendgaard NA (1988) Stellate ganglion innervation of the vertebrobasilar arterial system demonstrated in the rat with anterograde and retrograde WGA-HRP tracing. Brain Res 445:175–180

Bell RL, Atweh N, Ivy ME, Possenti P (2001) Traumatic and iatrogenic Horner syndrome: case reports and review of the literature. J Trauma Int Infec Critic Care 51:400–404

Bleys RLAW, Thrasivoulou C, Cowen T (2001) Cavernous sinus ganglia are sources for parasympathetic innervation of cerebral arteries in rat. J Cereb Blood Flow Metab 21:149–157

Boydell P (1995) Idiopathic Horners syndrome in the golden retriever. J Small Anim Pract 36:382–384

Bugge J (1971) The cephalic arterial system in new and old world hystricomorphs, and in bathyergoids, with special reference to the systematic classification of rodents. Acta Anat 80:516–536

Cardinali DP, Vacas MI, Gejman PV (1981) The sympathetic superior cervical ganglia as peripheral neuroendocrine centres. J Neural Transm 52:1–21

Casscells W (1992) Migration of smooth muscle and endothelial cells. Critical events in restenosis. Circulation 86:723–729

Clowes AW, Reidy MA, Clowes MM (1983) Kinetics of cellular proliferation after arterial injury. I. Smooth muscle growth in absence of endothelium. Lab Invest 49:327–333

Coutard M, Mertes P, Mairose P, Osborne-Pellegrin M, Michel J-B (2003) Arterial sympathetic innervation and cerebrovascular diseases in original rat models. Auton Neurosci 104:137–145

De Vriese B (1905) Sur la signification morphologique des artèries cérébrales. Arch Biol 21:357–457

Edvinsson L, Hara H, Uddman R (1989) Retrograde tracing of nerve fibres to the rat middle cerebral artery with true-blue: colocalisation with different peptides. J Cereb Blood Flow Metab 9:212–218

Fisher M, Ratan R (2003) New perspectives on developing acute stroke therapy. Ann Neurol 53:10–20

Gillilan L (1972) Blood supply to primitive mammalian brains. J Comp Neurol 145:209–222

Gladstone DJ, Black SE, Hakim AM (2002) Toward wisdom from failure: lessons from neuroprotective stroke trials and new therapeutic directions. Stroke 33:2123–2136

Handa Y, Caner H, Hayashi M, Tamamaki N, Nojyo Y (1990) The distribution pattern of sympathetic nerve fibers to the cerebral arterial system in rat as revealed by anterograde labeling with WGA-HRP. Exp Brain Res 82:493–498

Hardebo JE, Suzuki N, Owman C (1989) Origins of substance P and calcitonin gene-related peptide-containing nerves in the internal carotid artery of rat. Neurosci Lett 101:39–45

Herrera EA, McDonald DW (1984) The capybara. In: McDonald DW (ed) Encyclopaedia of mammals. George Allen and Unwin, London, pp 696–699

Islam S, Ribeiro AACM, Loesch A (2004) Basilar artery of the capybara (*Hydrochaeris hydrochaeris*): an ultrastructural study. Anat Histol Embryol 33:81–89

Lindner MD, Gribkoff VK, Donlan NA, Jones TA (2003) Long-lasting functional disabilities in middle-aged rats with small cerebral infarcts. J Neurosci 23:10913–10922

Loesch A, Gajkowska B, Dashwood MR, Fioretto ET, Gagliardo KM, Lima AR de, Ribeiro AACM (2005) Endothelin-1 and endothelin receptors in the basilar artery of the capybara. J Mol Histol 36:25–34

Malik N, Francis SE, Holt CM, Gunn J, Thomas GL, Shepherd L, Chamberlain J, Newman CMH, Cumberland DC, Crossman DC (1998) Apoptosis and cell proliferation after porcine coronary angioplasty. Circulation 96:1655–1657

Mione MC, Sancesario G, D'Angelo V, Bernardi G (1991) Increase of dopamine beta-hydroxylase immunoreactivity in non-noradrenergic nerves of rat cerebral arteries following long-term sympathectomy. Neurosci Lett 123:167–171

Navone F, Jahn R, Di Gioia G, Stuckenbrok H, Greengard P, De Camilli P (1986) Protein p38: an integral membrane protein specific for small vesicles of neurons and neuroendocrine cells. J Cell Biol 103:2511–2527

Nilges RG (1944) The arteries of the mammalian cornu ammonis. J Comp Neurol 80:117–190

Owman S, Edvinsson L (1977) Neurogenic control of the brain circulation: proceedings of international symposium held in the Wenner-Gren Center, Stockholm, June 22–24. Pergamon, Oxford and New York

Pickel VM, Joh TH, Reis DJ (1975) Ultrastructural localisation of tyrosine hydroxylase in noradrenergic neurons of the brain. Proc Natl Acad Sci USA 72:659–663

Reckziegel SH, Lindemann T, Campos R (2001) A systematic study of the brain base arteries in capybara (*Hydrochoerus hydrochaeris*). Braz J Morphol Sci 18:103–110

Reckziegel SH, Schneider FL, Edelweiss MIA, Lindemann T, Culau POV (2004) Anatomy of the caudal cerebral artery on the surface of capybara (*Hydrochoerus hydrochaeris*) brain. Braz J Morphol Sci 21:131–134

Ross R (1993) The pathogenesis of atherosclerosis: a perspective for the 1990s. Nature 362:801–809

Sadoshima S, Heistad D (1982) Sympathetic nerves protect the blood-brain barrier in stroke-prone spontaneously hypertensive rats. Hypertension 4:904–907

Sadoshima S, Busija D, Brody M, Heistad D (1981) Sympathetic nerves protect against stroke in stroke prone hypertensive rats. A preliminary report. Hypertension 3 (Suppl 1):124–127

Simons T, Ruskell GL (1988) Distribution and termination of trigeminal nerves to the cerebral arteries in monkeys. J Anat 59:57–71

Suzuki N, Hardebo JE, Owman C (1988) Origins and pathways of cerebrovascular vasoactive intestinal polypeptide-positive nerves in rat. J Cereb Blood Flow Metab 8:697–712

Tamamaki N, Nojyo Y (1987) Intracranial trajectories of sympathetic nerve fibers originating in the superior cervical ganglion in the rat: WGA-HRP anterograde labeling study. Brain Res 437:387–392

Thompson RJ, Doran JF, Jackson P, Dhillon AP, Rode J (1983) PGP 9.5 - a new marker for vertebrate neurons and neuroendocrine cells. Brain Res 278:224–228

Thrasivoulou C, Cowen T (1995) Regulation of rat sympathetic nerve density by target tissues and NGF in maturity and old age. Eur J Neurosci 7:381–387

Weidenman B, Frank WW (1985) Identification and localisation of synaptophysin, an integral membrane glycoprotein of Mr 38,000 characteristic of synaptic vesicles. Cell 41:1017–1028

Weninger WJ, Muller GB (1997) The sympathetic nerves of the parasellar region: pathways to the orbit and the brain. Acta Anat (Basel) 160:254–260